



Article

# Assessment of Climate Change Impacts in the North Adriatic Coastal Area. Part I: A Multi-Model Chain for the Definition of Climate Change Hazard Scenarios

Silvia Torresan <sup>1,2</sup>, Valentina Gallina <sup>1,2</sup>, Silvio Gualdi <sup>1</sup>, Debora Bellafiore <sup>3</sup>, Georg Umgiesser <sup>3,4</sup> , Sandro Carniel <sup>3</sup>, Mauro Sclavo <sup>3</sup>, Alvise Benetazzo <sup>3</sup>, Elisa Giubilato <sup>1</sup> and Andrea Critto <sup>1,2,\*</sup> 

<sup>1</sup> Centro-Euro Mediterraneo sui Cambiamenti Climatici (CMCC), Risk Assessment and Adaptation Strategies Division, via Augusto Imperatore 16, 73100 Lecce, Italy; torresan@unive.it (S.T.); vategallina@yahoo.it (V.G.); silvio.gualdi@ingv.it (S.G.); giubilato@unive.it (E.G.)

<sup>2</sup> Department of Environmental Sciences, Informatics and Statistics, University Ca' Foscari Venice, Via Torino 155, 30172 Venezia Mestre, Italy

<sup>3</sup> National Research Council of Italy (CNR), Institute of Marine Sciences (ISMAR), Castello 2737/f, 30122 Venice, Italy; debora.bellafiore@ve.ismar.cnr.it (D.B.); georg.umgiesser@ismar.cnr.it (G.U.); sandro.carniel@ismar.cnr.it (S.C.); mauro.sclavo@ismar.cnr.it (M.S.); alvise.benetazzo@ve.ismar.cnr.it (A.B.)

<sup>4</sup> Coastal Research and Planning Institute, CORPI, Klaipėda University, H. Manto 84, 92294 Klaipėda, Lithuania

\* Correspondence: critto@unive.it; Tel.: +39-(0)41-2348975; Fax: +39-(0)41-2348584

Received: 24 April 2019; Accepted: 28 May 2019; Published: 1 June 2019



**Abstract:** Climate scenarios produce climate change-related information and data at a geographical scale generally not useful for coastal planners to study impacts locally. To provide a suitable characterization of climate-related hazards in the North Adriatic Sea coast, a model chain, with progressively higher resolution was developed and implemented. It includes Global and Regional Circulation Models representing atmospheric and oceanic dynamics for the global and sub-continental domains, and hydrodynamic/wave models useful to analyze physical impacts of sea-level rise and coastal erosion at a sub-national/local scale. The model chain, integrating multiple types of numerical models running at different spatial scales, provides information about spatial and temporal patterns of relevant hazard metrics (e.g., sea temperature, atmospheric pressure, wave height), usable to represent climate-induced events causing potential environmental or socio-economic damages. Furthermore, it allows the discussion of some methodological problems concerning the application of climate scenarios and their dynamical downscaling to the assessment of the impacts in coastal zones. Based on a balanced across all energy sources emission scenario, the multi-model chain applied in the North Adriatic Sea allowed to assess the change in frequency of exceedance of wave height and bottom stress critical thresholds for sediment motion in the future scenario (2070–2100) compared to the reference period 1960 to 1990. As discussed in the paper, such projections can be used to develop coastal erosion hazard scenarios, which can then be applied to risk assessment studies, providing valuable information to mainstream climate change adaptation in coastal zone management.

**Keywords:** climate change; coastal hazards; multi-model chain; North Adriatic Sea

## 1. Introduction

Coastal areas represent vulnerable systems highly threatened by potential impacts of climate-induced hazards, such as frequent inundation of low-lying areas due to sea-level rise and increased rates of coastal erosion [1–3]. Sea-level rise could have devastating impacts on marine-coastal environments and

societies, contributing to the loss of lowlands and ecosystems, to damages for urban areas and economic activities [4,5]. Moreover, coastal erosion and human-induced pressures (e.g., urbanization, tourism, land-use changes), may exacerbate the loss of coastal areas particularly relevant for ecosystem services and human activities (e.g., wetlands, lagoons, and deltas, protected and agricultural areas) [6]. Therefore, there is an increasing need to understand how climate-change-induced impacts on wave climate, ocean circulation, and coastal erosion may affect the coastal areas.

Climate scenarios are widely considered a key tool for climate change impact and risk assessment [7]. They are used to detect possible changes in the climate and to identify various sources and types of uncertainty associated with the future evolution of our planet [8]. Examination of possible future climate scenarios, especially sea-level rise projections, is particularly relevant for the analysis of coastal flooding and erosion impacts.

To estimate changes in extreme water levels for the coastal assets in Dar es Salaam (Tanzania), Kebede and Nicholls [9], used global mean sea-level rise scenarios, also reflecting the post-AR4 projections (e.g., [10]). Moreover, Hinkel et al. [3] applied the Dynamic Interactive Vulnerability Assessment model (DIVA, [11]) for the analysis of coastal vulnerability to sea-level rise in Europe and Africa. Finally, the estimation of coastal erosion through the application of the Bruun's rule equation [6,11] was used to project changes in the profile of the shoreline based on global sea-level rise scenarios.

Climate change scenarios are commonly produced by Global and Regional Climate Models (GCMs, RCMs) at a relatively coarse spatial resolution (from hundreds to tens of kilometers) generally not suitable to assess the impacts at a local scale [8]. Therefore, methods are needed to bridge the gap between the large scale of climate scenarios and the local scale where climate impacts happen.

Downscaling methods allow obtaining high-resolution information about climate parameters from relatively coarse-resolution data (e.g., output of a GCM), which do not capture the effects of local/regional forcings [8]. The large-scale climate information is linked to the local scale with statistical models (i.e., statistical link between large and small scales features derived from observational datasets), or nesting high-resolution limited area models into GCMs [12].

Moreover, there is an increasing use of physically-based models, forced with downscaled or RCMs projections, to simulate the cascading effect of global warming on coastal processes (e.g., wave, currents, and shoreline dynamics), supporting maritime and coastal zone management [13]. Among these, Bellafiore et al. [14] assessed the relative capacity of different downscaled atmospheric datasets to reproduce wind and pressure statistics in the Adriatic region for the control period (1960–1990) evaluating their robustness for climate scenarios in this area. In another study [15], the change in the coastal climate, in terms of storm surge and wave height under high-resolution climate change forcings, has been studied.

The feasibility of a downscaling procedure from global to regional models aimed at assessing the wave climate of the Adriatic Sea has also been discussed in Benetazzo et al. [16].

Examples of the use of downscaling results in the Adriatic Sea are given by Lionello [17] who partially solved the spatial gap of information using regional modeling of waves and storm-surge, starting from GCMs. However, the results were used for the analysis of regional outputs without any detailed assessment of potential impacts and risks.

Even if these studies defined a complete climate change scenario for relevant physical processes (e.g., wave climate, current-sediment interactions, storm surge), they evidenced the need of integrating different models' results within a more comprehensive risk assessment framework, to provide local decision-makers with suitable information to define adaptation strategies.

Therefore, in the recent past, several attempts to apply multi-model chains for impact assessment studies have been started. In these approaches, a suite of high-resolution models (e.g., hydrodynamic, hydrologic or biogeochemical models) forced with the output of GCMs and RCMs were used to provide information about a multiplicity of regional/local stressors necessary to develop integrated risk and vulnerability assessments. To evaluate potential impacts on water quantity and quality

(e.g., groundwater level variation, variations of nitrate infiltration), Baruffi et al. [18] applied an integrated modeling approach in the Upper Veneto and Friuli plain (Italy). Lamon et al. [19] used an ensemble of oceanic and atmospheric models to identify precipitation, temperature, and evapotranspiration scenarios in the Gulf of Gabes (Tunisia). This was the first example of a model-chain applied to climate risk assessment in coastal areas, although no downscaling techniques were used in the experiment.

This paper aims to discuss a multi-model chain instrumental in evaluating the influence of global climate change on coastal risks (e.g., erosion, inundation) at the regional/sub-national scale. The chain provides information about spatial and temporal patterns of climate-related hazards (e.g., sea temperature, atmospheric pressure, sea-level, wave height, and bottom stress) that may be used within a coastal risk management framework, to identify environmental or socio-economic risks.

Particularly, the first aim of the paper is to present an integrated modeling methodology, putting together different types and scales of numerical models, towards the development of regional scale scenarios useful for climate change impact assessment. Second, the paper discusses the main problems arising from the use of the multi-model chain designed to characterize the complex interactions of climate change hazards in the North Adriatic (NA) coast, selected as a representative example of vulnerable Mediterranean coastal area.

The multi-model chain approach will be described in Section 3, after a brief introduction to the case study area (Section 2). Finally, the results of the model experiment, including climate change hazard maps, will be presented and discussed in Section 4.

## 2. Case Study

The coastal zone of Veneto and Friuli-Venezia Giulia regions borders the NA Sea (Figure 1) with about 2.400 km<sup>2</sup> of low-lying areas between the Po and the Isonzo river mouths. It is one of the Mediterranean areas more vulnerable to inundation due to the presence of large river mouths (e.g., Po, Adige, Brenta, Piave, Tagliamento); frequent storm surges flooding the city of Venice; relatively large tides compared to the rest of the Mediterranean; the presence of seiches, and increasing rates of relative sea-level rise due to both climate change and local subsidence [20,21]. Storm surge events are particularly relevant for the city of Venice, causing great damage to economic activities and cultural heritage [17]. An example is the extreme flood which happened in 1966, due to the co-occurrence of high tides, intensification of heavy pluvial events, and southeasterly winds [22].

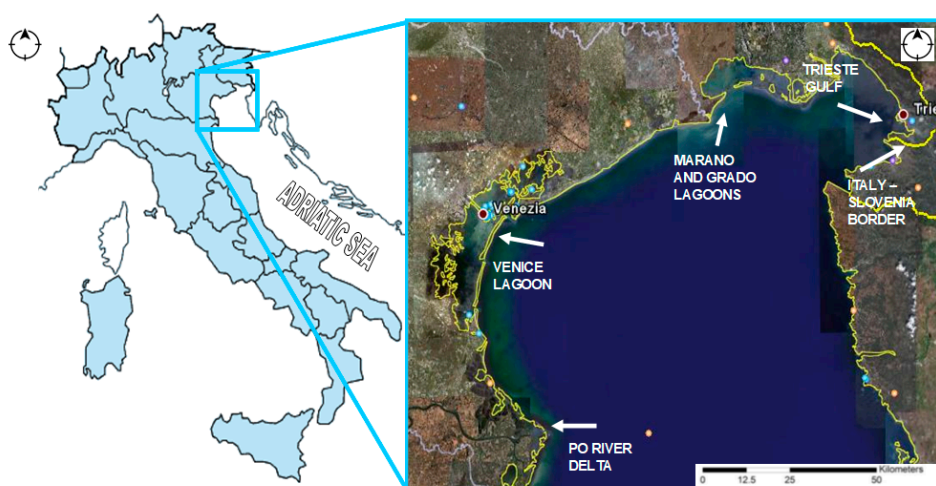


**Figure 1.** The case study area: the Northern Adriatic Sea and the coast of the Veneto and Friuli Venezia Giulia regions (Italy). (Adapted from google maps: maps.google.it).

Previous studies also agreed that the coastal area of the North Adriatic would be highly vulnerable to inundation due to global sea-level rise, particularly in the areas around the Po River Delta, that is located below the mean sea level and have been affected by natural and anthropic subsidence [23,24]. Furthermore, the analysis of observed sea level variations in this region showed higher relative sea-level rates (i.e., from 1.2 mm/year in Trieste to 2.5 mm/year in Venice) [25] compared to the average rates observed in the overall Mediterranean region (ranging from 1.1 mm/year to 1.3 mm/year) [26].

The coastal zone of the NA region is also particularly vulnerable to coastal inundation and erosion as proved by the significant implementation of artificial measures needed to prevent shoreline retreat (e.g., seawalls, breakwaters, and beach nourishment) [27–29]. Moreover, the NA oceanic circulation is typical for a semi-enclosed basin that experiences one of the highest tidal amplitudes in the Mediterranean [17].

From a climatic point of view, the case study area is characterized by relatively cold winters and warm summers. Annual mean temperatures range between 13 °C and 15 °C, and precipitations tend to occur during all the seasons, with a total annual mean precipitation ranging between 600 and 1100 mm. Winters are generally dry due to strong dry northeasterly winds (called Bora, see [30,31]), summers are characterized by moderate southeasterly winds (Scirocco, e.g., [32]) and sporadic rainstorms, while autumns and springs are prone to Atlantic and Mediterranean perturbations and different wind regimes ([www.arpa.veneto.it](http://www.arpa.veneto.it), [33]). A recent climatology of the Northern-Central Adriatic Sea, albeit including off-shore regions as well, can be found in Russo et al. [33].

Since the NA region is already experiencing several impacts related to sea-level rise (e.g., inundation and erosion) [34], and given its great environmental and socio-economic value, the NA coastal area was selected as a test case study for the model chain experiment.

### 3. The Multi-Model Chain Applied to Produce Climate Change Hazard Scenarios in the North Adriatic Coastal Area

This Section will describe the multi-model chain applied to develop climate-related hazard scenarios for the NA coast (Section 3.1). Each numerical model composing the multi-model chain will be analyzed separately (Sections 3.2–3.4).

#### 3.1. Multi-Model Chain Applied to the North Adriatic Sea

The multi-model chain developed in the NA coast includes different types of hydrodynamic and atmospheric models, with different spatial resolutions and setups simulating sea-level rise, wave fields, and bottom stresses processes. It has been used for the characterization of hazard scenarios within a broader risk assessment framework [35] developed to quantify climate change impacts and vulnerabilities in coastal areas.

Figure 2 shows the multi-model chain applied for the NA case study in its main components and interrelationships. First, climate change scenarios are used to force GCMs and RCMs, covering large spatial domains (i.e., global/sub-continental scale); then climate projections from GCMs and RCMs are used to force high-resolution hydrodynamic and wave models, simulating ocean dynamics and circulation processes in coastal waters, with spatial domains from the sub-national/regional to the local scale.

The overall chain is forced by radiative forcings obtained from the IPCC Special Report on Emissions Scenarios (SRES) scenario A1B [36], for the period 2070 to 2100. The A1B scenario belongs to the A1 storyline family describing a future world with very rapid economic growth. In this scenario, global population peaks around mid-century and declines thereafter, and new and more efficient technologies are rapidly introduced. Moreover, the A1B scenario predicts carbon dioxide emissions

increasing until around 2050 and then decreasing, and it assumes a balanced emphasis between fossil fuels and other energy sources. This scenario is used here, as in many other climate change impact studies, since it represents a sort of intermediate case between the intense A2 and the relatively weaker B1 emission scenarios.

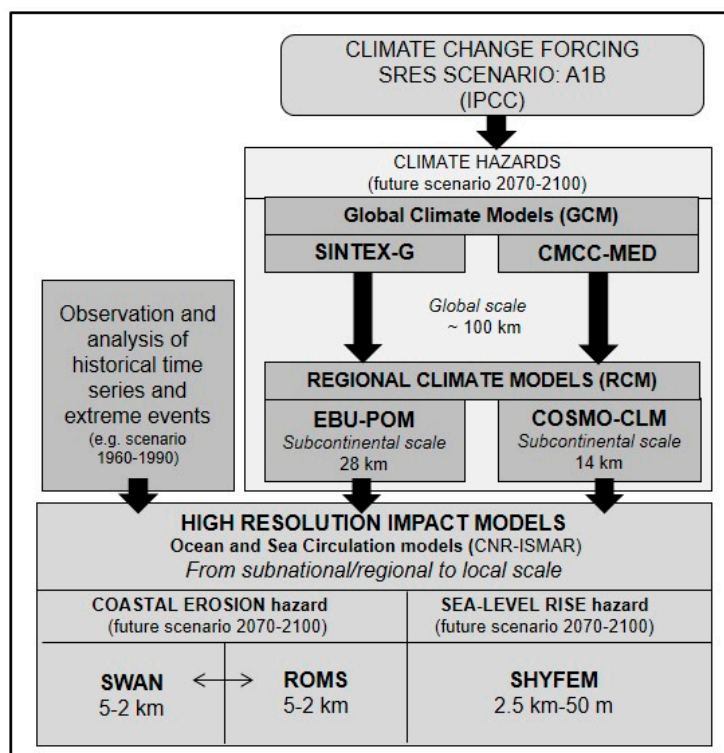


**Figure 2.** The multi-model chain applied to define climate change hazard scenarios in the North Adriatic coastal area. Names in brackets refer to partners who applied each model.

The A1B radiative forcing is used both by the GCM and the nested RCM. The outputs of the RCM are then used to construct downscaled climate hazard scenarios for the case study area. In fact, scenarios of temperature, precipitation, and wind variations are input for the suite of hydrodynamic and wave models running at higher spatial resolution (i.e., from the Adriatic to the NA scale) (Figure 2). The overall modeling approach can support the assessment of potential hazards related to climate change in coastal areas, such as the permanent inundation of low-lying areas due to sea-level rise and the coastal erosion related to changes in the circulation and waves pattern in the Adriatic Sea [35]. Climate-related hazards thus represent physical variations of the marine system (e.g., changes in temperature, pressure, sea-level) potentially harmful to coastal environments and assets. Specifically, sea-level rise hazards are associated with long-term sea physical alterations (e.g., water level, current velocity, water temperature) [37]; coastal erosion hazards arise from many climate-related factors including sea level, currents, wind and wave conditions as well as changing sediment rates triggering shoreline modifications and ecosystem loss [38].

### 3.2. Climate Scenarios

As shown in Figure 2, the climate change signal is provided by a set of climate models: an Atmosphere-Ocean Global Circulation Model (AOGCM) and a Regional Climate Model (RCM). The RCM is nested into the AOGCM and used to downscale the global climate change projections from a spatial resolution of about 100 km to a resolution of about 10 to 20 km, as more suitable input data of coastal and wave models at the end of the modeling chain.



Specifically, in this work two different sets of GCMs and RCMs have been used: The first set (hereafter MC1) is composed by the Eta Belgrade University–Princeton Ocean Models (EBU-POM) RCM nested into the Scale INTeraction Experiment SINTEX-G (SXG) AOGCM, and the second set (hereafter MC2) is composed by the COSMO-CLM (Consortium for Small-scale Modeling–Climate Limited area Modelling Community) RCM nested into the (CMCC-Med) global model developed by the Centro Euro-Mediterraneo sui Cambiamenti Climatici (CMCC) with a focus on the Mediterranean region (Med). The rationale for the use of two different sets of climate models to assess the possible climate change signal is to exploit the different capability that these models have demonstrated in reproducing the surface fields required for the application in the case study region [14].

A detailed description and discussion of the characteristics of these models are beyond the scope of the present paper. Thus, in the following, we will provide a brief description of their main, basic features relevant to the present discussion, and the references where the reader can find detailed information about the models and their performances in reproducing the observed global and regional climate.

SXG is a GCM with a relatively high horizontal resolution, suitable to produce long climate simulations and climate change projections [39,40]. For this work, climate simulations of the 20th and 21st centuries have been conducted integrating the model with forcing agents, which include greenhouse gases (CO<sub>2</sub>, CH<sub>4</sub>, N<sub>2</sub>O, and CFCs) and sulfate aerosols, as specified in the protocol for the 20C3M and A1B scenario experiments [36]. The model comprises the oceanic and atmospheric components. The oceanic component is the reference version 8.2 of the Océan Parallélisé (OPA) [40] with the ORCA2 global ocean configuration. The resolution is of about 2° × 2°, with increased meridional resolutions to 0.5° near the equator, and 31 vertical levels, 10 of which lie in the upper 100 m of the ocean. The atmospheric model component is the latest version of European Centre Hamburg Model 4 (ECHAM4) [41], here implemented with a horizontal resolution of approximately 100 km. The model outputs are used as input for the sub-continental climate model EBU-POM.

EBU-POM [42], is a regional ocean-atmosphere coupled model composed by the atmospheric component EBU (Eta Belgrade University) implemented with a spatial resolution of 0.125° (approximately 10 km) and 32 vertical levels, and the oceanic component POM (Princeton Ocean Models) with a horizontal resolution of 4 km and with 21 vertical levels. In this study, the spatial domain of the AORCM EBU-POM is the Mediterranean region, with a spatial resolution of approximately 28 km.

As shown in Figure 2, EBU-POM outputs produce climate scenarios used as surface forcings for the Shallow Water Hydrodynamic Finite Element Model (SHYFEM) hydrodynamic model, integrated with a very high spatial resolution in the Adriatic Sea (better described later).

The second modeling chain (MC2) is based on the set of climate models composed by the COSMO-CLM RCM, the climate version of the operational non-hydrostatic mesoscale weather forecast model COSMO (Consortium of Small-Scale Modeling, reference [43] nested into the CMCC-Med GCM.

The COSMO-CLM [44] is a finite difference atmosphere-only model that, in this numerical experiment, is implemented in the domain 2–20 E° and 39–52 N°, with a spatial resolution of approximately 14 km, 40 vertical levels [45]. The simulation is carried out with boundary conditions provided by the global climate model CMCC-MED [46,47], a coupled atmosphere–ocean general circulation model, composed by the atmospheric component ECHAM5 [48] with horizontal resolution of approximately 80 km and ocean component OPA-ORCA, as in SXG.

As presented in Figure 2, the outputs of the second set of climate models (CMCC-Med and COSMO-CLM) are used as boundary conditions for the Regional Ocean Modeling System (ROMS), as thoroughly described in Section 3.4. Two 30-year long periods covering the years 1965 to 1994 (control run) and 2070 to 2099 (future scenario, A1B) are extracted from the whole simulation that lasted from 1965 to 2099.

### 3.3. Sea-Level Rise Scenarios

The model used to produce the sea-level rise hazard scenarios is the Shallow Water Hydrodynamic Finite Element Model (SHYFEM) [49], which has been included in the model chain with the set MC1, as described in Section 3.2. SHYFEM is a free surface, primitive equation,  $z$  layer model that runs on an unstructured grid, and it has been shown to perform well in environments, such as lagoons, coastal marine areas, estuaries, and lakes [50]. The model consists of several modules: hydrodynamic, transport and diffusion, sediment transport, wave, and an ecologic module. In the present model chain, we used the hydrodynamic module implemented over the whole Adriatic Sea. The grid of SHYFEM is divided in triangles whose horizontal resolution varies from some kilometers in the Adriatic Sea to hundreds of meters in the coastal zone in the Northern end of the basin (i.e., from the regional to the local scale).

The outputs from the hydrodynamic module include water levels and current velocity.

The SHYFEM results that will be discussed here are based on simulations conducted using the 2D model version in barotropic mode, forced with the atmospheric pressure, and wind fields obtained from EBU-POM (MC1). The control period (1960–1990) was simulated as reference; two more simulations for the A1B IPCC scenario (2070–2100) were performed, laterally forcing the system at the Otranto Strait with a low sea-level rise (SLR) scenario (+20 cm in one century) and a high SLR scenario (+45 cm in one century).

### 3.4. Coastal Erosion Scenarios

To assess the coastal erosion hazard in the NA, in its last segment, the MC2 adopts a coupled model system already successfully applied in several applications within the Adriatic Sea [31,51]. It consists of the oceanic circulation model ROMS (<http://www.myroms.org>), a state-of-the-art hydrodynamic model that solves finite difference approximations of the three-dimensional Reynolds-averaged equations for conservation of mass, momentum, and heat. ROMS was two-way coupled with the wave model Simulating WAVes Nearshore (SWAN; [52]) and linked to a sediment transport module. Benetazzo et al. [53] provide a detailed description of this system.

Numerical simulations of the Adriatic Sea were conducted with the coupled ROMS-SWAN modeling system at high horizontal resolution (~2 km up to 5 km), for the two time-slice periods considered here: the reference period 1960–1990 and the projection period 2070–2100 for the A1B scenario.

The surface fluxes used to force the model have been obtained from the Coupled Ocean-Atmosphere Response Experiment (COARE)(COARE) bulk flux algorithms [54], where shortwave radiation, wind, air temperature, humidity, and atmospheric pressure were provided by the CMCC-CM/COSMO-CLM model chain (MC2) and the sea surface temperature (SST) obtained from ROMS.

Daily averaged time series of river discharges from the Po River were supplied. In addition, to better account for the impact on coastal circulation, the monthly mean value outflows of other 48 rivers [31] were prescribed.

At the southern Adriatic open boundary (namely Otranto Straits) both tidal elevation and currents for the main tidal components (M2, S2, K1, O1) were specified, the values resulting from a finite element model of the whole Mediterranean [55]. The barotropic open boundary conditions are from Flather [56] for the 2-D momentum and Chapman [57] for the tidal elevation. For 3-D passive tracers and baroclinic fields, the Orlanski [58] radiation condition is prescribed.

The same wind fields adopted to drive the upper ocean circulation were used to force SWAN. Resulting bottom wave parameters (orbital motion and wave period near the bottom) were used by ROMS-SWAN to compute combined wave-current bottom stress (for details see [13,59]).

This model can be used to determine impacts in coastal zones, such as coastal erosion, offshore sedimentation, and water quality variations. High-resolution ROMS-SWAN applications can account for the reproduction of near-shore processes, including wave–current interactions, sediment morphology, and a wetting and drying algorithm [13]. However, in this configuration, the computing resources required for long climate integrations become prohibitive. Therefore, in this work, we used the significant wave height and wave–current bottom stress as useful proxies for coastal erosion. These data have been produced for the reference period (1960–1990) and the future scenario (2070–2100) as daily averaged in the NA coast, without a detailed resolution of the lagoon areas [60].

More information about the technical features of the NA multi-model chain, including the hazard metrics used for the construction of climate change hazard maps, the domain and spatial/temporal resolution of the models, is attached as supplementary material of this paper (Table S1).

As described in the following section, the information of the multi-model chain was used to construct climate change hazard scenarios. Each hazard scenario represent the physical evidence of climatic variability or changes (e.g., changes in temperature and precipitation patterns, sea-level rise inundation, wave storms) and has the potential to cause environmental or socio-economic risks on the coast, to be further investigated with exposure and vulnerability assessment in the North Adriatic coastal zone [35].

#### 4. Results and Discussion

This Section analyzes the trends of variables resulting from the multi-model chain (Figure 2) and summarized in Table S1 for the A1B scenario in the future timeframe 2070 to 2100.

First, the main features of the climate change signal projected by the two sets of climate models MC1 (SXG and EBU-POM) and MC2 (CMCC-Med and COMSO-CLM) are introduced and compared with the current scenario 1960 to 1990. Then, representative statistics produced by physical impact models (i.e., SHYFEM and ROMS-SWAN) and climate-related hazard scenarios, and maps for the timeframe 2070 to 2100 are presented and discussed.

As far as climate parameters are concerned, we show the changes in the near surface temperature projected by the global models and some information on wind produced by the regional EBU-POM and COSMO-CLM.

To assess the capability of the global models (SXG and CMCC-Med) to reproduce the main basic features of the observed climate, with a special focus on the region of interest for this study, the results obtained from the climate simulations for the reference period (1961–1990 and referred to as CTRL simulation) are compared with atmospheric re-analyses. Specifically, the model results were compared with the 2-meter air temperature (T2m) obtained from the European Centre for Medium-Range Weather Forecasts (ECMWF) Re-Analyses (ERA-40; more information available online at <http://www.ecmwf.int/research/era>). For the sake of brevity, in the following, we will show and discuss the results obtained from the climate simulations and climate change projections performed with the SXG GCM. Similar results have been obtained with the CMCC-Med model, especially regarding the climate change signal. The reader who is interested in gaining more insight into the performances and the climate change signal produced by these models should refer to Gualdi et al. [39], Bellucci et al. [40], Scoccimarro et al. [46] and Gualdi et al. [47] and references therein.

Figure 3 shows the 2-meter temperature (T2m) winter (DJF) and summer (JJA) means as obtained from the ECMWF re-analyses (left column, panels a and d) and from the global model SXG simulations. The panels in the middle column (panels b and e), labeled as CTRL, show the seasonal means as obtained from the simulated reference period (1961–1990) and the panels in the right column (panels c and f) show the differences between the projected mean temperature for the period 2071 to 2100 according to the A1B scenario and the reference period. The comparison with the re-analyses indicates that the SXG model captures reasonably well the main features of the observed mean low-level temperature, especially during the winter season (DJF, upper panels).



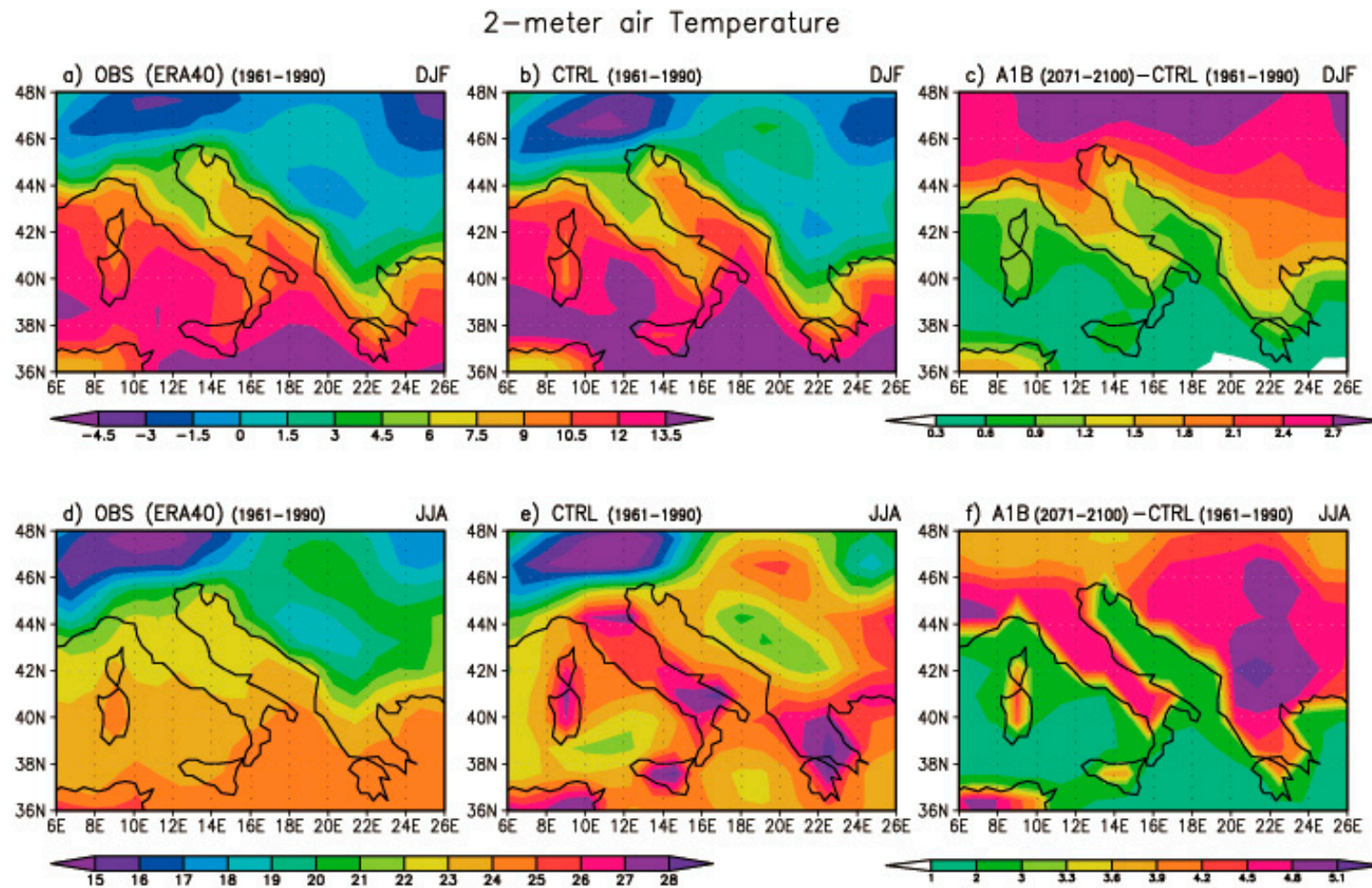


**Figure 3.** 2-meter air temperature (T2 m) seasonal means, units °C. Left column panels: seasonal means as obtained from the ECMWF Re-Analyses for the period 1961 to 1990, for northern winter (DJF, panel (a)) and northern summer (JJA, panel (d)). Central column panels: seasonal means as obtained from the global coupled model SXG for the period 1961–1990, for northern winter (DJF, panel (b)) and northern summer (JJA, panel (e)). Right column panels: differences between the seasonal means from the last part of the 21st century (2071–2100, panel (c)) and from the reference period (1961–1990, panel (f)).

During northern summer (JJA, lower panels), the simulated temperature is warmer than the re-analyses over a large part of the domain, and especially over the Italian Peninsula and the Balkans. Over the Alps, on the other hand, the model temperature is cooler than observed, producing a larger modeled southern temperature gradient.

The differences between projected (A1B scenario) and reference seasonal mean temperature (right panels) show substantial warming during both season and over the entire domain of interest here. The projected mean temperature increase at the end of the 21st century is more pronounced in summer (panel f), when the warming over the Balkans can be as large as about 5 °C. In winter (panel c), the warming (up to about 2.7 °C) is larger over the northern part of the domain.

We have also compared the seasonal means of the low-level wind (at 950 hPa) as obtained from the ECMWF re-analyses, from the CTRL simulation performed with the SXG and the CMCC-Med models for the reference period and the differences between the seasonal means for the last part of the 21st century in the A1B scenario and the reference period. Figure 4 shows the results obtained from the observations (left panels), and from the SXG model (control simulation—central panels—and differences between the future scenario and the reference period—right panels). The results obtained from the CMCC-Med model are similar to those shown for the SXG model and, for the sake of brevity, we do not show them. Furthermore, in this case, the model seems to reproduce the basic gross features of the observed climate, such as, for example, the intense Etesian winds that blow during northern summer over the south-eastern part of the domain (Figure 4, lower left and central panels). In contrast, the simulated mean wind during the northern winter in the CTRL runs exhibits some substantial differences compared to observations (Figure 4, upper left and central panels). In both the global models, the simulated wind, in fact, tends to be too strong and predominantly westerly over most of the domain, whereas the re-analyses show much weaker wind in the northern part of the considered region, with some easterlies over the NA basin.

The low-level wind change projected according to the A1B scenario with both models (SXG—Figure 4, right panels—and CMCC-CM, not shown) exhibits an increase of the anticyclonic circulation over the whole domain during northern winter, which leads to reinforced north-easterlies over most of the Adriatic basin, especially in its southern part. This result appears to be in good agreement with those obtained from other studies (e.g., [47] and references therein). During summer (Figure 4, bottom right panel), the projected change appears to be less homogeneous over the considered area, however, also in this season, the Adriatic Sea seems to be characterized by stronger north-easterlies low-level winds.

Furthermore, the result of the climate change projections (i.e., temperature) in Figure 3 is mostly consistent with those obtained in several previous analyses of the climate change signal in the Southern Europe—Mediterranean area (e.g., [14,47] and references therein) conducted using climate models with different characteristics. Therefore, it is reasonable to conclude that the main basic features of the projected changes discussed here seem to be considerably robust and, in their general aspects, mostly independent from the climate model used.

Using as climate forcings the variables supplied by the regional climate model EBU-POM (i.e., atmospheric pressure and winds) presented before, the SHYFEM model produces data about water level projections for the whole Adriatic Sea in the future timeframe 2070 to 2100.

Based on the overall data provided by the SHYFEM model for the thirty-year period 2070 to 2100, the selection of the more appropriate statistics representing sea-level rise hazard scenarios to be used in risk assessment was focused on the year 2100, as it represents the worst sea-level rise conditions (i.e., the more precautionary conditions) for the future century.

Specifically, the SHYFEM simulations were performed imposing as boundary conditions at the Otranto strait two sea-level rise scenarios: a low sea-level rise scenario equal to 20 cm and a high sea-level rise scenario equal to 45 cm. The boundary conditions at Otranto were set considering the low and high IPCC global sea-level rise projections for the year 2100 according to the emission scenario A1B and assuming a linear sea-level rise trend for the future period 2070 to 2100. It has to be

pointed out that, even if low and high range scenarios have been selected from IPCC, these do by no means represent the highest possible values. Some additional ranges of sea-level rise can be found in Umgiesser et al. [49] that do not exclude a rise of more than 1 meter in the Mediterranean Sea.

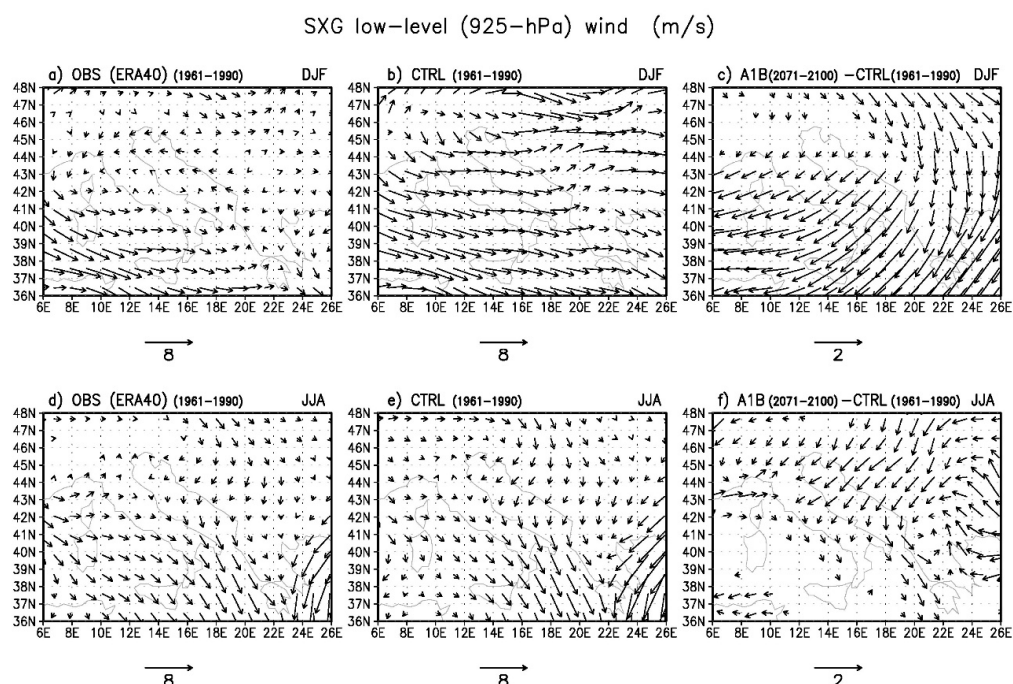


**Figure 4.** Seasonal means of the low-level (925-hPa) wind over the domain of interest as obtained from the European Centre for Medium-Range Weather Forecasts (ECMWF) re-analyses (left panels a) and d)), and from the SXG model (central b) and e) and right c) and f) panels). The upper panels (a), b), c)) show the winter (December–February, DJF) seasonal means, whereas the lower panels (d), e), f)) show the summer (June–August, JJA) seasonal means. The central panels (b) and e)) show the simulated seasonal mean wind for the reference period (1961–1990), whereas the right panels (c) and f)) show the difference between the seasonal means from the A1B scenario simulations for the 1971 to 2100 period and the reference period (1961–1990). The reference arrows are also shown and indicate a wind velocity of 8 m/s for the observations (re-analyses) and for the model results (left and central panels). The reference arrow for the difference between the projected and control simulation is 2 m/s.

The results of this assessment, attached in the supplementary material, include: a low sea-level rise hazard map representing the water levels averaged over the last simulated year (2100), according to a sea-level rise at Otranto equal to 20 cm (Figure S1a); a high sea-level rise hazard map representing the water levels according to a sea-level rise at Otranto equal to 45 cm (Figure S1b).

As shown in Figure S1a,b, most of the area of the NA Sea (i.e., from Po River Delta to the Italy–Slovenia border) is characterized by an average water level ranging from 0.164 m to 0.169 m for the low sea-level rise map and from 0.414 m to 0.419 m for the high sea-level rise map.

Since the range of data variability for the SHYFEM dots adjoining to the shoreline (about 1280) is very low (Figure S1a,b), the maximum value was selected as the more precautionary statistic to be used for the construction of sea-level rise hazard scenarios for the case study area. Accordingly, with an upper approximation, the selected statistics correspond to 17 cm for the low sea-level rise scenario and to 42 cm for the high sea-level rise scenario.

The low and high sea-level rise hazard maps can be used for the assessment of low-lying coastal areas (and vulnerable targets) that can be inundated by sea-level rise in view of climate change. Specifically, in recent studies [35,61], the sea-level rise hazard maps were used to evaluate the territory that can be lost (i.e., permanently inundated by sea-level rise) and for the assessment of related risks for different vulnerable receptors (e.g., beaches, wetlands, protected areas, agricultural and urban areas).



It is important to note that only IPCC scenarios have been used in the NA example, even if they do not include mass addition of polar ice melting [62].

These scenarios are therefore necessarily on the lower spectrum of the possible sea-level rise evolution. As shown in the results, sea-levels in the NA are always lower than the values imposed at the Otranto strait. This is due to meteorological conditions of atmospheric pressure and wind regimes. The results show an average water level that is consistently lower by about 3 cm with respect to the southern Adriatic Sea.

The construction of coastal erosion maps is based on the output provided by the coupled system ROMS-SWAN (Section 3.4), supplying information about several variables relevant to study coastal erosion processes (i.e., bottom stress, water velocity, wave height, and wave energy). Two significant hazard metrics were selected to map erosion hazard in the NA coast: wave height and bottom stress. The reasons for this choice are both scientific (the bottom stress fields integrate the information of flow velocity, the significant wave height summarize the wave energy information) and strategic, being one goal of the present work to present a procedure readily employed and exported in many other contexts. In fact, it should be underlined that bottom stresses (albeit induced by pure current) and significant wave height fields (albeit resulting from a stand-alone wave model) are indeed among the most common parameters that can be provided to Decision Support System (DSS) experts in many coastal regions. To summarize the significant amount of information provided by the ROMS-SWAN system (Section 3.4), a procedure was therefore proposed for the identification of extreme events on the base of obtained wave fields and bottom stresses. The extreme events were identified using a threshold and then calculating the number of events over the selected threshold (de facto, a “peak over threshold” approach, see [63]). At the international level, the 90th, 93rd, or 95th percentiles are widely used as thresholds for the identification of extreme events [64,65]. In general, an advantage of the use of percentiles, rather than absolute thresholds, is that they account for regional climate differences [66].

For the NA coast, the 90th percentile of the reference scenario (1960–1990) for each coastal grid point was selected as a reasonable threshold for the identification of relevant extreme events for coastal erosion. The thresholds for the coastal erosion impact range from 0.60 to 1.40 m for wave height and from 0.01 to 0.40 N/m<sup>2</sup> for bottom stress, and the mean values (i.e., 0.97 m and to 0.15 N/m<sup>2</sup>, respectively) were considered as representative thresholds in this work.

The statistic selected for the construction of coastal erosion hazard scenarios corresponds to the number of wave height and bottom stress events that exceed the selected thresholds in each season for the future scenario 2070 to 2100 in each station. The four analyzed seasons correspond to the following trimesters: January/February/March; April/May/June; July/August/September, October/November/December. Finally, the hazard scenarios for the NA area were obtained by the linear interpolation of the seasonal average values above described. Accordingly, eight seasonal hazard scenarios were produced for the period 2070 to 2100 in the NA area (Figure 5), showing how the situation changes in the future scenario compared to the reference one. Each model used in the modeling chain to simulate climate and hydrodynamic processes was already validated and discussed through the comparison with observed data for a control period [14,38,42].

Hazard classes (i.e., ranges of events exceeding the threshold calculated in the reference scenario) were defined for the four seasons using the equal interval method. Concerning the spatial variance of extreme wave height events in each season of the scenario 2070 to 2100, the winter trimester (Figure 5a) shows a medium hazard class in the Friuli Venezia Giulia coast, a high class in the area between Grado-Marano and Venice lagoon, and a very high class from Venice to the Po Delta. The spring and summer seasons (Figure 5b,c) are characterized by very low hazard classes. This means that in these seasons, there is a lower number of wave events exceeding the threshold compared to other trimesters in the case study area. Finally, the autumn season (Figure 5d) shows higher hazard scores in the northern half part of the territory and relatively lower scores in the southern. These results are in good qualitative agreement with other studies focused on future wave-climate scenarios in the Adriatic Sea, such as those proposed by Benetazzo et al. [16].

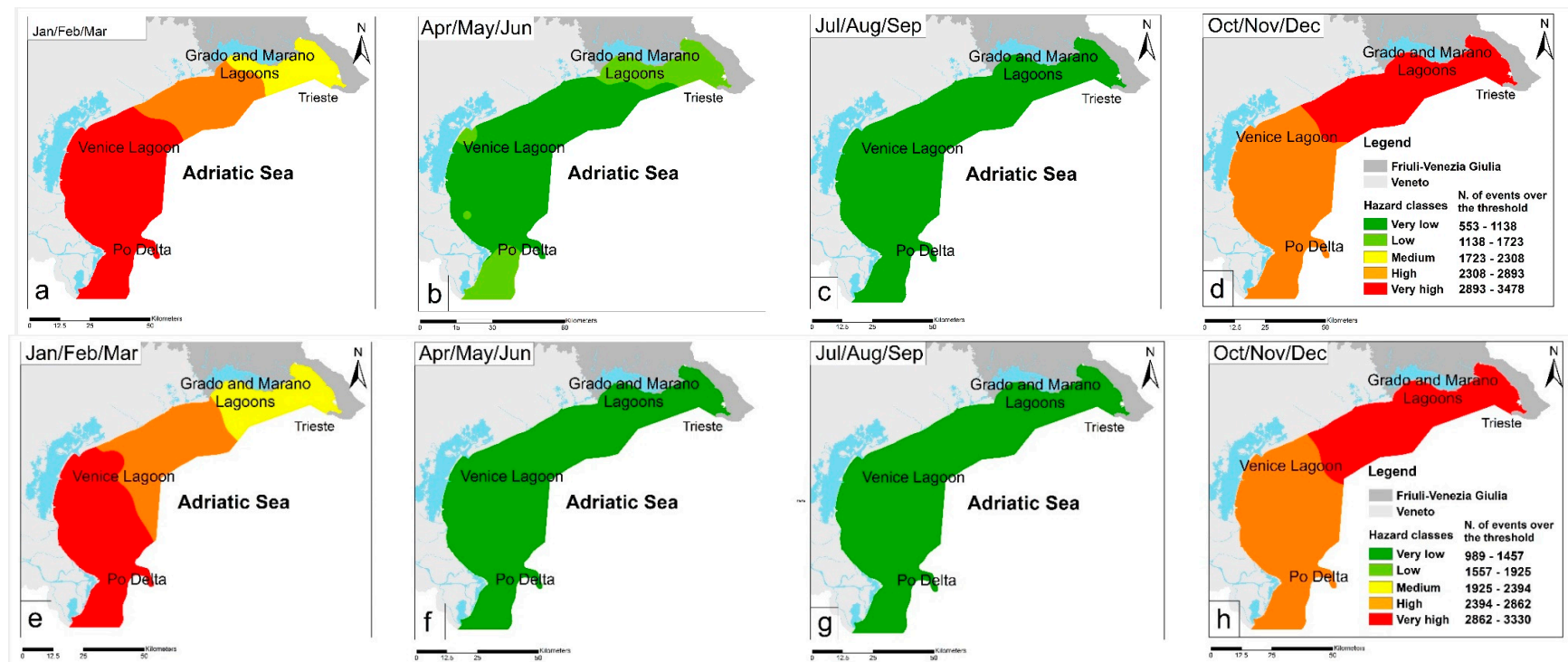


**Figure 5.** Hazard Maps representing the number of events exceeding the wave height (a–d) and bottom stress (e–h) thresholds (i.e., 0.97 m and 0.15 N/m<sup>2</sup>, respectively) as resulting from the coupled ROMS-SWAN system in the future scenario 2070 to 2100, for the four seasons: January/February/March, April/May/June, July/August/September, October/November/December. The spatial variance of bottom stress events in the four seasons for 2070 to 2100 shows that there is a decrease of hazard classes (i.e., from very high to medium) from south to north in winter (Figure 5e). Spring (Figure 5f) is mainly represented by the very low hazard class, except for few low hazard areas in the southern and northern zones of the NA. Finally, summer (Figure 5g) is interested by very low hazard class in the whole case study, while the autumn season (Figure 5h) is characterized by high hazard class in the southern area and very high hazard class in the northern one.



According to Gallina et al. [35], the bottom stress and wave height hazard metrics can be integrated with information about the presence of artificial protections and the distance from the shoreline identifying and classifying areas potentially exposed to higher rates of erosion processes under changing climate. The map of areas exposed to coastal erosion is then combined with information about the receptors' susceptibility to obtain a relative estimate of coastal parcels and elements at higher risk from coastal erosion in the NA coast.

## 5. Conclusions

The main objective of this paper was to illustrate a methodology for the assessment of climate change impacts in coastal zones based on a modeling chain composed of different types and spatial scales of numerical models. As a case study, the modeling chain has been implemented in the North Adriatic region, representing a first attempt in joining different models (i.e., climate models, hydrodynamic, and wave models) to consistently describe how climate scenarios can influence relevant drivers of coastal changes at the regional scale.

Further experiments are needed to reach definitive results, but the outcomes of this first work indicate that the proposed approach can represent a solution to bridge the gap between coarse information produced by global climate change projections and the detailed information required to investigate the regional impacts of climate change on coastal dynamics [14]. Moreover, it provides relevant hazard metrics (e.g., sea-level rise, wave heights, bottom stress) with a spatial resolution (up to 2 km) suitable to analyze the potential physical impacts of climate change in coastal areas (e.g., areas more prone to inundation or erosion).

However, the level of uncertainty exhibited by state-of-the-art climate models—especially when dealing with storminess situations—suggests that the results produced by these assessments have to be taken with caution. In fact, the systematic errors introduced by the climate simulations can have significant repercussions on the results of the proposed model chain and should be reduced by applying bias correction techniques (as is generally done in local impact studies). Moreover, the modeling chain generates a cascade of uncertainty related to the assumptions about the radiative forcing and anthropogenic emissions, as well as the choice of climate and hydrodynamic models and their parameterization.

Clearly, more model development, tuning, and data acquisitions are needed for a more careful evaluation of parameters, such as critical shear stress, nearshore wave height. Nevertheless, the approach shown by this model-chain effort is built in such a way that it can promptly benefit from rapid improvements of the model products currently employed.

As demonstrated in the accompanying paper Gallina et al. (submitted in the same special issue), the hazard metrics provided by the multi-model chain can be easily integrated with information about land use/land cover, the presence of natural ecosystems or man-made structures, to provide significant advancements in the assessment of risks and vulnerability due to climate-related hazards at the regional scale, to finally mainstream climate adaptation planning in coastal zones.

**Supplementary Materials:** The following are available online at <http://www.mdpi.com/2073-4441/11/6/1157/s1>, Figure S1: Hazard Maps representing the Adriatic sea-level rise (SLR) for the year 2100. Sea-level changes are simulated by the SHYFEM model according to a SLR at Otranto of 20 cm (low scenario, a); and of 45 cm (b, high scenario). Table S1: Summary of the technical features of the multi-model chain applied to develop climate change hazard scenarios in the North Adriatic coastal areas.

**Author Contributions:** Conceptualization, S.T., V.G., E.G. and A.C.; Data curation, S.G., D.B., S.C. and A.B.; Formal analysis, S.T., S.G., D.B., G.U., S.C., M.S. and A.B.; Methodology, S.T., V.G., S.G., D.B., S.C., E.G. and A.C.; Supervision, G.U., M.S. and A.C.; Writing—original draft, S.T., V.G., S.G., D.B., S.C., G.U. and A.C.; Writing—review & editing, S.T., V.G., S.G., D.B., S.C., A.B. and A.C.

**Funding:** The research leading to these results has received funding from the Italian Ministry of Education, University and Research and the Italian Ministry of Environment, Land, and Sea under GEMINA project.

**Acknowledgments:** Bucchignani Edoardo and Djurdjevic Vladimir are thanked for having made the climate model data available.

**Conflicts of Interest:** The authors declare no conflict of interest.

## References

1. EEA. *The Changing Faces of Europe's Coastal Areas*; EEA Report No 6/2006; European Environment Agency: Copenhagen, Denmark, 2006; Available online: [www.eea.europa.eu/publications/eea\\_report\\_2006\\_6](http://www.eea.europa.eu/publications/eea_report_2006_6) (accessed on 30 May 2019).
2. Nicholls, R.J.; Cazenave, A. Sea-Level Rise and Its Impact on Coastal Zones. *Science* **2010**, *328*, 1517–1520. [[CrossRef](#)] [[PubMed](#)]
3. Hinkel, J.; Brown, S.; Nicholls, R.J.; Vafeidis, A.T.; Kebede, A.S. Sea-level rise impacts on Africa and the effects of mitigation and adaptation: An application of DIVA. *Reg. Environ. Chang.* **2011**, *12*, 207–224. [[CrossRef](#)]
4. Pachauri, R.K.; Allen, M.R.; Barros, V.R.; Broome, J.; Cramer, W.; Christ, R.; Church, J.A.; Clarke, L.; Qin, D.; Purnamita, D.; et al. *Climate Change 2014: Synthesis Report; Contribution of Working Groups I, II and III to the Fifth Assessment Report of the Intergovernmental Panel on Climate Change*; Intergovernmental Panel on Climate Change: Geneva, Switzerland, 2014.
5. Ward, P.J.; Marfai, M.A.; Yulianto, F.; Hizbaron, D.R.; Aerts, J.C.J.H. Coastal inundation and damage exposure estimation: A case study for Jakarta. *Nat Hazards* **2010**. [[CrossRef](#)]
6. Sharples, C. *Indicative Mapping of Tasmanian Coastal vulnerability to Climate Change and Sea Level Rise: Explanatory Report*, 2nd ed.; Department of Primary Industries, Water & Environment: Tasmania, Australia, 2006; 112p.
7. Wilby, R.L.; Troni, J.; Biot, Y.; Tedd, L.; Hewitson, B.C.; Smithe, D.M.; Suttonf, R.T. A review of climate risk information for adaptation and development planning. *Int. J. Climatol.* **2009**, *29*, 1193–1215. [[CrossRef](#)]
8. UKCIP. *Climate Adaptation: Risk, Uncertainty and Decision-Making*; Willows, R., Connell, R., Eds.; UKCIP: Oxford, UK, 2003; p. 166.
9. Kebede, A.S.; Nicholls, R.J. Exposure and vulnerability to climate extremes: Population and asset exposure to coastal flooding in Dar es Salaam, Tanzania. *Reg. Environ. Chang.* **2011**, *12*, 81–94. [[CrossRef](#)]
10. Ganopolski, A.; Rahmstorf, S. Rapid changes of glacial climate simulated in a coupled climate model. *Nature* **2001**, *409*, 153–158. [[CrossRef](#)]
11. Vafeidis, A.T.; Boot, G.; Cox, J.; Maatens, R.; Mcfadden, L.; Nicholls, R.J.; Tol, R.S.J. The DIVA Database Documentation. Technical Report; Available online: <http://wedocs.unep.org/xmlui/handle/20.500.11822/15051> (accessed on 1 June 2019).
12. IPCC-TGICA. *General Guidelines on the Use of Scenario Data for Climate Impact and Adaptation Assessment. Version 2*; Prepared by T.R. Carter on behalf of the Intergovernmental Panel on Climate Change, Task Group on Data and Scenario Support for Impact and Climate Assessment; IPCC: Geneva, Switzerland, 2007; 66p.
13. Carniel, S.; Sclavo, M.; Archetti, R. Towards validating a last generation, integrated wave-current-sediment numerical model in coastal regions using video measurements. *Oceanol. Hydrobiol. Stud.* **2011**, *40*, 11–20. [[CrossRef](#)]
14. Bellafiore, D.; Bucchignani, E.; Gualdi, S.; Carniel, S.; Djurdjevic, V.; Umgiesser, G. Assessment of meteorological climate model inputs for coastal hydrodynamics modelling. *Ocean Dyn.* **2012**, *62*, 555–568. [[CrossRef](#)]
15. Weisse, R.; Bellafiore, D.; Menéndez, M.; Méndez, F.; Nicholls, R.J.; Umgiesser, G.; Willems, P. Changing extreme sea levels along European coasts. *Coast. Eng.* **2013**, *87*, 4–14. [[CrossRef](#)]
16. Benetazzo, A.; Carniel, S.; Sclavo, M.; Bucchignani, E.; Ricchi, A. Wave climate of the Adriatic Sea: A future scenario simulation. *Nat. Hazards Earth Syst. Sci.* **2012**, *12*, 1–11. [[CrossRef](#)]
17. Lionello, P. The climate of the Venetian and North Adriatic region: Variability, trends and future change. *Phys. Chem. Earth Parts A/B/C* **2005**, *40–41*, 1–8. [[CrossRef](#)]
18. Baruffi, F.; Cisotto, A.; Cimolino, A.; Ferri, M.; Monego, M.; Norbiato, D.; Cappelletto, M.; Bisaglia, M.; Pretner, A.; Galli, A.; et al. Climate change impacts assessment on Veneto and Friuli plain groundwater. Part I: An integrate modeling approach for hazard scenario construction. *Sci. Total Environ.* **2012**, *440*, 154–166. [[CrossRef](#)] [[PubMed](#)]
19. Lamon, L.; Rizzi, J.; Bonaduce, A.; Dubois, C.; Lazzari, P.; Ghenim, L.; Gana, S.; Somot, S.; Li, L.; Melaku Canu, D.; et al. An ensemble of models for identifying climate change scenarios in the Gulf of Gabes, Tunisia. *Reg. Environ. Chang.* **2013**, *14*, 31–40. [[CrossRef](#)]

20. Bondesan, M.; Castiglioni, G.B.; Elmi, C.; Gabbianelli, G.; Marocco, R.; Pirazzoli, P.A.; Tomasin, A. Coastal areas at risk from storm surges and sea-level rise in Northeastern Italy. *J. Coast. Res.* **1995**, *11*, 1354–1379.
21. Tosi, L.; Carbognin, L.; Teatini, P.; Rosselli, R.; Gasparetto-Stori, G. The ISES Project subsidence monitoring of the catchment basin south of the Venice Lagoon (Italy). In Proceedings of the Sixth International Symposium on Land Subsidence, Ravenna, Italy, 24–29 September 2000; Volume II, pp. 113–126.
22. De Zolt, P.; Lionello, A.; Nuhu, A. Tomasin. The disastrous storm of 4 November 1966 on Italy. *Nat. Hazards Earth Syst. Sci.* **2006**, *6*, 861–879. [[CrossRef](#)]
23. Pirazzoli, P.A. A review of possible eustatic, isostatic and tectonic contributions in eight late-Holocene relative sea-level histories from the Mediterranean area. *Quat. Sci. Rev.* **2005**, *24*, 1989–2001. [[CrossRef](#)]
24. Antonioli, F.; Anzidei, M.; Amorosi, A.; Lo Presti, V.; Mastronuzzi, G.; Deiana, G.; De Falco, G.; Fontana, A.; Fontolan, G.; Lisco, S.; et al. Sea-level rise and potential drowning of the Italian coastal plains: Flooding risk scenarios for 2100. *Quat. Sci. Rev.* **2017**, *158*, 29–43. [[CrossRef](#)]
25. Antonioli, F.; Silenzi, S. Variazioni relative del livello del mare e vulnerabilità delle pianure costiere italiane. *Quad. Della Soc. Geol. Ital.* **2007**, *2*, 1–29.
26. Tsimplis, M.N.; Spencer, N.E. Collection and analysis of monthly mean sea level data in the Mediterranean and the Black Sea. *J. Coast. Res.* **1997**, *13*, 534–544.
27. Cecconi, G.; Ardone, V. La fonte di approvvigionamento della sabbia nel ripascimento dei litorali veneti. Presented at the della Costa ligure, Regione Liguria, Genova, Italy, 2–4 February 2000.
28. Visintini Romanin, M.; Rismondo, A.; Scarton, F.; Leita, L. Interventi per il recupero morfologico della laguna di Venezia. La barena Fossei Est in laguna Sud. *Quad. Trimest.* **2000**, *3/4*, 3–35.
29. FVG Region. Piano di gestione del SIC IT3320037 Laguna di Grado e Marano. Carta delle aree di tutela e di intervento scala 1:50000. Available online: [http://www.regione.fvg.it/rafv/export/sites/default/RAFVG/ambiente-territorio/tutela-ambiente-gestione-risorse-naturali/FOGLIA203/allegati/documenti\\_tecnici/PdG\\_Laguna\\_testo.pdf](http://www.regione.fvg.it/rafv/export/sites/default/RAFVG/ambiente-territorio/tutela-ambiente-gestione-risorse-naturali/FOGLIA203/allegati/documenti_tecnici/PdG_Laguna_testo.pdf) (accessed on 1 June 2019).
30. Dorman, C.E.; Carniel, S.; Cavaleri, L.; Sclavo, M.; Chiggiato, J.; Doyle, J.; Haack, T.; Pullen, J.; Grbec, B.; Vilibić, I.; et al. February 2003 marine atmospheric conditions and the Bora over the Northern Adriatic. *J. Geophys. Res. Ocean* **2006**, *111*, C03S03. [[CrossRef](#)]
31. Boldrin, A.; Carniel, S.; Giani, M.; Marini, M.; Bernardi Aubry, F.; Campanelli, A.; Grilli, F.; Russo, A. Effects of bora wind on physical and biogeochemical properties of stratified waters in the northern Adriatic. *J. Geophys. Res.* **2009**, *114*, C08S92. [[CrossRef](#)]
32. Signell, R.P.; Carniel, S.; Cavaleri, L.; Chiggiato, J.; Doyle, J.; Pullen, J.; Sclavo, M. Assessment of wind quality for oceanographic modeling in semi-enclosed basins. *J. Mar. Syst.* **2005**, *53*, 217–233. [[CrossRef](#)]
33. Russo, A.; Carniel, S.; Sclavo, M.; Krzelj, M. Climatology of the Northern-Central Adriatic Sea. In *Modern Climatology*; Wang, S.-Y., Ed.; InTech: Rijeka, Croatia, 2012; ISBN 978-953-51-0095-9. [[CrossRef](#)]
34. Bonaldo, D.; Antonioli, F.; Archetti, R.; Bezzi, A.; Correggiari, A.; Davolio, S.; de Falco, G.; Fantini, M.; Fontolan, G.; Furlani, S.; et al. Integrating multidisciplinary instruments for assessing coastal vulnerability to erosion and sea level rise: Lessons and challenges from the Adriatic Sea, Italy. *J. Coast. Conserv.* **2018**, *23*, 19–37. [[CrossRef](#)]
35. Gallina, V.; Torresan, S.; Zabeo, A.; Carniel, S.; Sclavo, M.; Pizzol, L.; Marcomini, A.; Critto, A. Assessment of climate change impacts in the North Adriatic coastal area. Part II: Coastal erosion impacts at the regional scale. *Water* **2019**, *11*, 1300. [[CrossRef](#)]
36. Nakićenović, N.; Alcamo, J.; Davis, G.; de Vries, H.J.M.; Fenhann, J.; Gaffin, S.; Gregory, K.; Grubler, A.; Jung, T.Y.; Kram, T.; et al. *Special Report on Emissions Scenarios*; Intergovernmental Panel on Climate Change: Geneva, Switzerland; Cambridge University Press: Cambridge, UK, 2000.
37. IPCC. *Climate Change 2007: The Physical Science Basis. Summary for Policymakers Contribution of Working Group I to the Fourth Assessment Report*; Intergovernmental Panel on Climate Change: Geneva, Switzerland, 2007.
38. Wong, P.P.; ILosada, J.; Gattuso, J.-P.; Hinkel, J.; Khattabi, A.; McInnes, K.L.; Saito, Y.; Sallenger, A. Coastal systems and low-lying areas. In *Climate Change 2014: Impacts, Adaptation, and Vulnerability. Part A: Global and Sectoral Aspects. Contribution of Working Group II to the Fifth Assessment Report of the Intergovernmental Panel on Climate Change*; Field, C.B., Barros, V.R., Dokken, D.J., Mach, K.J., Mastrandrea, M.D., Bilir, T.E., Chatterjee, M., Ebi, K.L., Estrada, Y.O., Genova, R.C., et al., Eds.; Cambridge University Press: Cambridge, UK; New York, NY, USA, 2014; pp. 361–409.

39. Gualdi, S.; Rajkovic, B.; Djurdjevic, V.; Castellari, S.; Scoccimarro, E.; Navarra, A.; Dacic, M. SINTA—Simulations of Climate Change in the Mediterranean Area—Final Scientific Report. Earth-Prints T.R. 2008, p. 70. Available online: <http://www.earth-prints.org/> (accessed on 30 May 2019).
40. Bellucci, A.; Gualdi, S.; Scoccimarro, E.; Navarra, A. NAO-Ocean Circulation Interactions in a Coupled General Circulation Model. *Clim. Dyn.* **2008**, *31*, 759–777. [[CrossRef](#)]
41. Madec, G.; Delecluse, P.; Imbard, M.; Levy, C. *OPA 8.1 Ocean General Circulation Model Reference Manual*; Internal Rep. 11; Institute Pierre Simon Laplace: Paris, France, 1998; p. 91.
42. Roeckner, E.; Oberhuber, J.M.; Bacher, A.; Christoph, M.; Kirchner, I. ENSO variability and atmospheric response in a global coupled atmosphere-ocean GCM. *Clim. Dyn.* **1996**, *12*, 737–754. [[CrossRef](#)]
43. Djurdjevic, V.; Rajkovic, B. Development of the EBU-POM coupled regional climate model and results from climate change experiments. In *Advances in Environmental Modeling and Measurements*; Mihajlovic, T.D., Lalic, B., Eds.; Nova Publishers: Hauppauge, NY, USA, 2010.
44. Steppeler, J.; Doms, G.; Schättler, U.; Bitzer, H.; Gassmann, A.; Damrath, U.; Gregoric, G. Meso-gamma scale forecasts using the nonhydrostatic model LM. *Meteorol. Atmos. Phys.* **2003**, *82*, 75–96. [[CrossRef](#)]
45. Rockel, B.; Geyer, B. The performance of the regional climate model CLM in different Climate regions, based on the example of precipitation. *Meteorol. Z.* **2008**, *17*, 487–498. [[CrossRef](#)]
46. Bucchignani, E.; Mercogliano, P.; Montesarchio, M.; Manzi, M.; Zollo, A. Performance evaluation of COSMO-CLM over Italy and climate projections for the XXI century. Climate change and its implications on ecosystem and society. In Proceedings of the I SISC (Società Italiana di Scienze del Clima) Conference, Lecce, Italy, 23–24 September 2013; pp. 78–89, ISBN 978-88-97666-08-0.
47. Scoccimarro, E.; Gualdi, S.; Bellucci, A.; Sanna, A.; Fogli, P.G.; Manzini, E.; Vichi, M.; Oddo, P.; Navarra, A. Effects of Tropical Cyclones on Ocean Heat Transport in a High Resolution Coupled General Circulation Model. *J. Clim.* **2011**, *24*, 4368–4384. [[CrossRef](#)]
48. Gualdi, S.; Somot, S.; Li, L.; Artale, V.; Adani, M. The CIRCE simulations: A new set of regional climate change projections performed with a realistic representation of the Mediterranean Sea. *Bull. Am. Meteorol. Soc.* **2013**, *94*, 65–81. [[CrossRef](#)]
49. Roeckner, E.; Brokopf, R.; Esch, M.; Giorgetta, M.; Hagemann, S.; Kornblueh, L. Sensitivity of simulated climate to horizontal and vertical resolution in the ECHAM5 atmosphere model. *J. Clim.* **2006**, *19*, 3771–3791. [[CrossRef](#)]
50. Umgiesser, G.; Anderson, J.B.; Artale, V.; Breil, M.; Gualdi, S.; Lionello, P.; Marinova, N.; Orlić, M.; Pirazzoli, P.; Rahmstorf, S.; et al. From Global to Regional: Local Sea Level Rise Scenarios—Focus on the Mediterranean Sea and the Adriatic Sea. In Proceedings of the Workshop organized by UNESCO Venice Office and ISMAR-CNR, Venice, Italy, 22–23 November 2010.
51. De Pascalis, F.; Pérez-Ruzafa, A.; Gilabert, J.; Marcos, C.; Umgiesser, G. Climate change response of the Mar Menor coastal lagoon (Spain) using a hydrodynamic finite element model, Estuarine. *Coast. Shelf Sci.* **2012**, in press. [[CrossRef](#)]
52. Carniel, S.; Warner, J.C.; Chiggiato, J.; Sclavo, M. Investigating the impact of surface wave breaking on modelling the trajectories of drifters in the Northern Adriatic Sea during a wind-storm event. *Ocean Model.* **2009**, *30*, 225–239. [[CrossRef](#)]
53. Booij, N.; Ris, R.C.; Holthuijsen, L.H. A third-generation wave model for coastal regions. Part I—Model description and validation. *J. Geophys. Res.* **1999**, *104*, 7649–7666. [[CrossRef](#)]
54. Benetazzo, A.; Carniel, S.; Sclavo, M.; Bergamasco, A. Wave-current interaction: Effect on the wave field in a semi-enclosed basin. *Ocean Model.* **2013**, *70*, 152–165. [[CrossRef](#)]
55. Fairall, C.W.; Bradley, E.F.; Hare, J.E.; Grachev, A.A.; Edson, J.B. Bulk Parameterization of Air–Sea Fluxes: Updates and Verification for the COARE Algorithm. *J. Clim.* **2003**, *16*, 571–591. [[CrossRef](#)]
56. Cushman-Roisin, B.; Naimie, C.E. A 3D finite-element model of the Adriatic tides. *J. Mar. Syst.* **2002**, *37*, 279–297. [[CrossRef](#)]
57. Flather, R.A. A tidal model of the northwest European continental shelf. *Mem. De La Soc. R. De Sci. De Liege* **1976**, *6*, 141–164.
58. Chapman, D.C. Numerical treatment of cross-shelf open boundaries in a barotropic coastal ocean model. *J. Phys. Oceanogr.* **1985**, *15*, 1060–1075. [[CrossRef](#)]
59. Orlandi, I. A simple boundary condition for unbounded hyperbolic flows. *J. Comp. Sci.* **1976**, *21*, 251–269. [[CrossRef](#)]

60. Harris, C.K.; Sherwood, C.R.; Signell, R.P.; Bever, A.J.; Warner, J.C. Sediment dispersal in the northwestern Adriatic Sea. *J. Geophys. Res. Oceans* **2008**, *113*. [[CrossRef](#)]
61. Bergamasco, A.; Carniel, S.; Pastres, R.; Pecelik, G. A unified approach to the modelling of the Venice Lagoon-Adriatic Sea ecosystem. *Estuar. Coast. Shelf Sci.* **1998**, *46*, 483–492. [[CrossRef](#)]
62. Torresan, S. Development of a Regional Risk Assessment Methodology for Climate Change Impact Assessment and Management in Coastal Zones. Ph.D. Thesis, University Ca'Foscari, Venice, Italy, 2012.
63. Rahmstorf, S. A semi-empirical approach to projecting future sea-level rise. *Science* **2007**, *315*, 368–370. [[CrossRef](#)]
64. Martucci, G.; Carniel, S.; Chiggiato, J.; Sclavo, M.; Lionello, P.; Galati, M.B. Statistical trend analysis and extreme distribution of significant wave height from 1958 to 1999—An application to the Italian Seas. *Ocean Sci.* **2009**, *6*, 525–538. [[CrossRef](#)]
65. Vinoth, J.; Young, I.R. Global Estimates of Extreme Wind Speed and Wave Height. *Am. Meteorol. Soc.* **2011**. [[CrossRef](#)]
66. William, G.J.; Hegerl, G.C.; Holland, G.J.; Knutson, T.R.; Mearns, L.O.; Stouffer, R.J.; Webster, P.J.; Wehner, M.F.; Zwiers, F.W. Observed Changes in Weather and Climate Extremes. In *Synthesis and Assessment Product 3.3 Report by the U.S. Climate Change Science Program and the Subcommittee on Global Change Research*; Karl, R., Meehl, G.A., Miller, C.D., Hassol, S.J., Waple, A.M., Murray, W.L., Eds.; Available online: <https://www.climatecommunication.org/wp-content/uploads/2012/01/climateextremes.pdf> (accessed on 1 June 2019).



© 2019 by the authors. Licensee MDPI, Basel, Switzerland. This article is an open access article distributed under the terms and conditions of the Creative Commons Attribution (CC BY) license (<http://creativecommons.org/licenses/by/4.0/>).